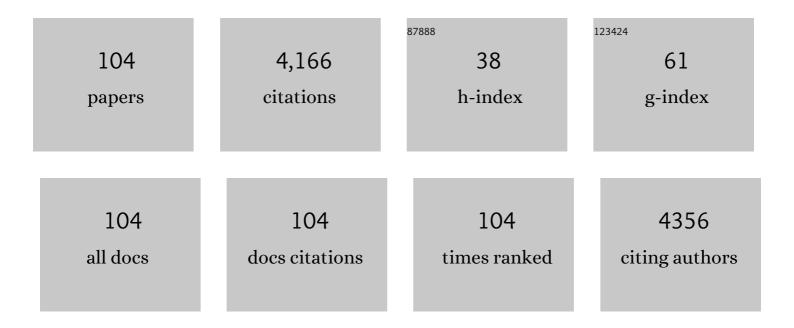
List of Publications by Year in descending order

Source: https://exaly.com/author-pdf/1007877/publications.pdf Version: 2024-02-01



7ньшлясти

#	Article	IF	CITATIONS
1	A luminescent lanthanide MOF for selectively and ultra-high sensitively detecting Pb <sup>2+</sup> ions in aqueous solution. Journal of Materials Chemistry A, 2017, 5, 10200-10205.	10.3	225
2	An ultrastable zinc( <scp>ii</scp> )–organic framework as a recyclable multi-responsive luminescent sensor for Cr( <scp>iii</scp> ), Cr( <scp>vi</scp> ) and 4-nitrophenol in the aqueous phase with high selectivity and sensitivity. Journal of Materials Chemistry A, 2017, 5, 20035-20043.	10.3	215
3	Controllable Synthesis of a Smart Multifunctional Nanoscale Metal–Organic Framework for Magnetic Resonance/Optical Imaging and Targeted Drug Delivery. ACS Applied Materials & Interfaces, 2017, 9, 3455-3462.	8.0	192
4	Ultrastable 1D Europium Complex for Simultaneous and Quantitative Sensing of Cr(III) and Cr(VI) Ions in Aqueous Solution with High Selectivity and Sensitivity. Inorganic Chemistry, 2017, 56, 4197-4205.	4.0	169
5	Fabrication of functional hollow microspheres constructed from MOF shells: Promising drug delivery systems with high loading capacity and targeted transport. Scientific Reports, 2016, 6, 37705.	3.3	117
6	Zinc( <scp>ii</scp> )–organic framework as a multi-responsive photoluminescence sensor for efficient and recyclable detection of pesticide 2,6-dichloro-4-nitroaniline, Fe( <scp>iii</scp> ) and Cr( <scp>vi</scp> ). New Journal of Chemistry, 2019, 43, 2353-2361.	2.8	113
7	A microporous metal–organic open framework containing uncoordinated carbonyl groups as postsynthetic modification sites for cation exchange and Tb3+ sensing. Chemical Communications, 2013, 49, 6897.	4.1	112
8	Enhanced visible light photocatalytic activity in BiOCl/SnO <sub>2</sub> : heterojunction of two wide band-gap semiconductors. RSC Advances, 2015, 5, 22740-22752.	3.6	107
9	Size and surface controllable metal–organic frameworks (MOFs) for fluorescence imaging and cancer therapy. Nanoscale, 2018, 10, 6205-6211.	5.6	103
10	Postsynthetic Metalation Metal–Organic Framework as a Fluorescent Probe for the Ultrasensitive and Reversible Detection of PO <sub>4</sub> <sup>3–</sup> lons. Inorganic Chemistry, 2018, 57, 10525-10532.	4.0	102
11	Fabrication of porous metal–organic frameworks via a mixed-ligand strategy for highly selective and efficient dye adsorption in aqueous solution. CrystEngComm, 2015, 17, 6037-6043.	2.6	100
12	A multi-chemosensor based on Zn-MOF: Ratio-dependent color transition detection of Hg (II) and highly sensitive sensor of Cr (VI). Sensors and Actuators B: Chemical, 2018, 269, 164-172.	7.8	99
13	Fabrication of a Luminescence-Silent System Based on a Post-Synthetic Modification Cd-MOFs: A Highly Selective and Sensitive Turn-on Luminescent Probe for Ascorbic Acid Detection. Inorganic Chemistry, 2019, 58, 6167-6174.	4.0	90
14	A Discrete Dysprosium Trigonal Prism Showing Singleâ€Molecule Magnet Behaviour. Chemistry - A European Journal, 2012, 18, 442-445.	3.3	80
15	Enhanced electrocatalytic nitrogen reduction reaction performance by interfacial engineering of MOF-based sulfides FeNi2S4/NiS hetero-interface. Applied Catalysis B: Environmental, 2021, 287, 119956.	20.2	75
16	A highly selective turn-on luminescent logic gates probe based on post-synthetic MOF for aspartic acid detection. Sensors and Actuators B: Chemical, 2019, 284, 91-95.	7.8	74
17	A luminescent terbium MOF containing uncoordinated carboxyl groups exhibits highly selective sensing for Fe <sup>3+</sup> ions. RSC Advances, 2014, 4, 55252-55255.	3.6	72
18	Utilizing 3d–4f Magnetic Interaction to Slow the Magnetic Relaxation of Heterometallic Complexes. Inorganic Chemistry, 2015, 54, 4337-4344.	4.0	72

#	Article	IF	CITATIONS
19	A gadolinium MOF acting as a multi-responsive and highly selective luminescent sensor for detecting o-, m-, and p-nitrophenol and Fe <sup>3+</sup> ions in the aqueous phase. RSC Advances, 2016, 6, 61725-61731.	3.6	70
20	Construction of Metallosupramolecular Coordination Complexes: From Lanthanide Helicates to Octahedral Cages Showing Single-Molecule Magnet Behavior. Inorganic Chemistry, 2019, 58, 3167-3174.	4.0	69
21	Fabrication of a magnetic nanocomposite photocatalysts Fe3O4@ZIF-67 for degradation of dyes in water under visible light irradiation. Journal of Solid State Chemistry, 2017, 255, 150-156.	2.9	67
22	One-pot synthesis of hierarchical-pore metal–organic frameworks for drug delivery and fluorescent imaging. CrystEngComm, 2018, 20, 1087-1093.	2.6	67
23	Constructing Bi24O31Cl10/BiOCl heterojunction via a simple thermal annealing route for achieving enhanced photocatalytic activity and selectivity. Scientific Reports, 2016, 6, 28689.	3.3	64
24	Stable Europium-based Metal–Organic Frameworks for Naked-eye Ultrasensitive Detecting Fluoroquinolones Antibiotics. Inorganic Chemistry, 2021, 60, 5282-5289.	4.0	64
25	Two Locally Chiral Dysprosium Compounds with Salenâ€Type Ligands That Show Slow Magnetic Relaxation Behavior. European Journal of Inorganic Chemistry, 2013, 2013, 1351-1357.	2.0	62
26	Waste control by waste: Fenton–like oxidation of phenol over Cu modified ZSM–5 from coal gangue. Science of the Total Environment, 2019, 683, 638-647.	8.0	59
27	Intriguing pH-modulated Luminescence Chameleon System based on Postsynthetic Modified Dual-emitting Eu <sup>3+</sup> @Mn-MOF and Its Application for Histidine Chemosensor. Inorganic Chemistry, 2020, 59, 6390-6397.	4.0	59
28	3D Ln <sup>III</sup> -MOFs: slow magnetic relaxation and highly sensitive luminescence detection of Fe <sup>3+</sup> and ketones. Dalton Transactions, 2018, 47, 8972-8982.	3.3	56
29	A stable europium metal–organic framework as a dual-functional luminescent sensor for quantitatively detecting temperature and humidity. Dalton Transactions, 2016, 45, 18450-18454.	3.3	54
30	Insight to unprecedented catalytic activity of double-nitrogen defective metal-free catalyst: Key role of coal gangue. Applied Catalysis B: Environmental, 2020, 263, 118316.	20.2	51
31	Synthesizing Bi2O3/BiOCl heterojunctions by partial conversion of BiOCl. Journal of Materials Science, 2017, 52, 2117-2130.	3.7	49
32	Synthesis of carbon doped Bi2MoO6 for enhanced photocatalytic performance and tumor photodynamic therapy efficiency. Applied Surface Science, 2019, 465, 369-382.	6.1	48
33	Hollow structural metal–organic frameworks exhibit high drug loading capacity, targeted delivery and magnetic resonance/optical multimodal imaging. Dalton Transactions, 2019, 48, 17291-17297.	3.3	43
34	Eu3+ doped bismuth metal-organic frameworks with ultrahigh fluorescence quantum yield and act as ratiometric turn-on sensor for histidine detection. Sensors and Actuators B: Chemical, 2021, 336, 129753.	7.8	43
35	A terbium metal–organic framework with stable luminescent emission in a wide pH range that acts as a quantitative detection material for nitroaromatics. RSC Advances, 2015, 5, 48574-48579.	3.6	41
36	Self-doping for visible light photocatalytic purposes: construction of SiO <sub>2</sub> /SnO <sub>2</sub> /SnO <sub>2</sub> :Sn <sup>2+</sup> nanostructures with tunable optical and photocatalytic performance. RSC Advances, 2014, 4, 30820.	3.6	40

#	Article	IF	CITATIONS
37	A luminescent europium MOF containing Lewis basic pyridyl site for highly selective sensing of o-, m- and p-nitrophenol. RSC Advances, 2015, 5, 86614-86619.	3.6	39
38	A diabolo-shaped Dy9 cluster: synthesis, crystal structure and magnetic properties. Dalton Transactions, 2011, 40, 6440.	3.3	38
39	Outstanding Drug-Loading/Release Capacity of Hollow Fe-Metal–Organic Framework-Based Microcapsules: A Potential Multifunctional Drug-Delivery Platform. Inorganic Chemistry, 2021, 60, 1664-1671.	4.0	37
40	A highly selective and sensitive fluorescent sensor based on Tb <sup>3+</sup> -functionalized MOFs to determine arginine in urine: a potential application for the diagnosis of cystinuria. Analyst, The, 2019, 144, 5875-5881.	3.5	32
41	A Promising White-Light-Emitting Material Constructed from Encapsulating Eu3+/Tb3+ Hybrid Ions into a Robust Microporous Metal-Organic Framework. European Journal of Inorganic Chemistry, 2016, 2016, 2837-2842.	2.0	31
42	Halloysite derived 1D mesoporous tubular g-C3N4: Synergy of template effect and associated carbon for boosting photocatalytic performance toward tetracycline removal. Applied Clay Science, 2021, 213, 106238.	5.2	30
43	Halloysite Nanotubes as an Effective and Recyclable Adsorbent for Removal of Low-Concentration Antibiotics Ciprofloxacin. Minerals (Basel, Switzerland), 2018, 8, 387.	2.0	29
44	Synthesis and Characterization of Modified BiOCl and Their Application in Adsorption of Low-Concentration Dyes from Aqueous Solution. Nanoscale Research Letters, 2018, 13, 69.	5.7	27
45	A metal–organic framework constructed by a viologen-derived ligand: photochromism and discernible detection of volatile amine vapors. New Journal of Chemistry, 2019, 43, 9032-9038.	2.8	27
46	A water stable Eu( <scp>iii</scp> )–organic framework as a recyclable multi-responsive luminescent sensor for efficient detection of <i>p</i> -aminophenol in simulated urine, and Mn <sup>VII</sup> and Cr <sup>VI</sup> anions in aqueous solutions. Dalton Transactions, 2021, 50, 5236-5243.	3.3	27
47	Natural kaolin derived stable SBA-15 as a support for Fe/BiOCl: a novel and efficient Fenton-like catalyst for the degradation of 2-nitrophenol. RSC Advances, 2015, 5, 36948-36956.	3.6	26
48	White-light emitting materials with tunable luminescence based on steady Eu( <scp>iii</scp> ) doping of Tb( <scp>iii</scp> ) metal–organic frameworks. RSC Advances, 2016, 6, 25689-25694.	3.6	26
49	A 3D porous luminescent terbium metal-organic framework for selective sensing of F â^ in aqueous solution. Inorganic Chemistry Communication, 2017, 80, 53-57.	3.9	26
50	Near-Infrared Emissive Lanthanide Metal–Organic Frameworks for Targeted Biological Imaging and pH-Controlled Chemotherapy. ACS Applied Materials & Interfaces, 2021, 13, 59164-59173.	8.0	25
51	Highly Selective and Sensitive Detection of PO <sub>4</sub> <sup>3–</sup> lons in Aqueous Solution by a Luminescent Terbium Metal–Organic Framework. ACS Omega, 2019, 4, 16378-16384.	3.5	24
52	A white-light-emitting lanthanide metal–organic framework for luminescence turn-off sensing of MnO <sub>4</sub> <sup>â^'</sup> and turn-on sensing of folic acid and construction of a "turn-on plus―system. New Journal of Chemistry, 2020, 44, 10239-10249.	2.8	24
53	An investigation into the magnetic interactions in a series of Dy <sub>2</sub> single-molecule magnets. Dalton Transactions, 2020, 49, 10477-10485.	3.3	23
54	Homochiral crystallization of single-stranded helical coordination polymers: generated by the structure of auxiliary ligands or spontaneous symmetry breaking. CrystEngComm, 2013, 15, 5598.	2.6	22

#	Article	IF	CITATIONS
55	Water-stable Cd( <scp>ii</scp> )/Zn( <scp>ii</scp> ) coordination polymers as recyclable luminescent sensors for detecting hippuric acid in simulated urine for indexing toluene exposure with high selectivity, sensitivity and fast response. Dalton Transactions, 2021, 50, 553-561.	3.3	21
56	Five new 2D and 3D coordination polymers based on two new multifunctional pyridyl–tricarboxylate ligands: hydrothermal syntheses, structural diversity, luminescent and magnetic properties. RSC Advances, 2017, 7, 19039-19049.	3.6	20
57	Significantly enhancing the lithium-ion conductivity of solid-state electrolytes <i>via</i> a strategy for fabricating hollow metal–organic frameworks. Chemical Communications, 2020, 56, 14629-14632.	4.1	20
58	Indium oxide/Halloysite composite as highly efficient adsorbent for tetracycline Removal: Key roles of hydroxyl groups and interfacial interaction. Applied Surface Science, 2021, 566, 150708.	6.1	20
59	Structural determinations and magnetic studies of two new binuclear complexes: azido-bridged Ni(II) dimer and di-(µ-hydroxo)-bridged Cr(III) dimer. Journal of Coordination Chemistry, 2010, 63, 3441-3452.	2.2	19
60	Structure control and crystal-to-crystal transformation for two series of lanthanide–organic coordination polymers. CrystEngComm, 2013, 15, 8522.	2.6	19
61	Hypersensitive Self-Referencing Detection Traces of Water in Ethyl Alcohol by Dual-Emission Lanthanide Metal-Organic Frameworks. European Journal of Inorganic Chemistry, 2018, 2018, 1998-2003.	2.0	18
62	Enhanced photocatalytic activity of Bi12O17Cl2 preferentially oriented growth along [200] with various surfactants. Journal of Materials Science, 2018, 53, 14217-14230.	3.7	17
63	Significantly Enhancing the Lithium Ionic Conductivity of Metal–Organic Frameworks via a Postsynthetic Modification Strategy. Langmuir, 2021, 37, 3922-3928.	3.5	17
64	Crystal structure and magnetic properties of two dinuclear iron(III) complexes with multidentate Schiff-base ligands. Journal of Coordination Chemistry, 2011, 64, 3531-3540.	2.2	16
65	In situ growth of metal–organic frameworks (MOFs) on the surface of other MOFs: a new strategy for constructing magnetic resonance/optical dual mode imaging materials. Dalton Transactions, 2017, 46, 13686-13689.	3.3	16
66	Eu(III)-organic framework as a multi-responsive photoluminescence sensor for efficient detection of 1-naphthol, Fe3+ and MnO4â^' in water. Inorganica Chimica Acta, 2020, 511, 119843.	2.4	16
67	Zinc(II) and Nickel(II) Complexes Based on Schiff Base Ligands: Synthesis, Crystal Structure, Luminescent and Magnetic Properties. Zeitschrift Fur Anorganische Und Allgemeine Chemie, 2014, 640, 462-468.	1.2	15
68	A chemically stable europium metal-organic framework for bifunctional chemical sensor and recyclable on–off–on vapor response. Journal of Solid State Chemistry, 2017, 251, 243-247.	2.9	14
69	Mannitol-assisted synthesis of ultrathin Bi2MoO6 architectures: excellent selective adsorption and photocatalytic performance. Journal of Nanoparticle Research, 2019, 21, 1.	1.9	13
70	Unprecedented catalytic activity of coal gangue toward environmental remediation: Key role of hydroxyl groups. Chemical Engineering Journal, 2020, 380, 122432.	12.7	13
71	Proton conduction studies on four porous and nonporous coordination polymers with different acidities and water uptake. CrystEngComm, 2020, 22, 6935-6946.	2.6	13
72	Fabrication of a "turn-on―type enantioselective fluorescence sensor <i>via</i> a modified achiral MOF: applications for synchronous detection of phenylalaninol enantiomers. Analyst, The, 2021, 146, 937-942.	3.5	12

#	Article	IF	CITATIONS
73	Metal–organic framework-encapsulated nanoparticles for synergetic chemo/chemodynamic therapy with targeted H <sub>2</sub> O <sub>2</sub> self-supply. Dalton Transactions, 2021, 50, 15870-15877.	3.3	12
74	A series of [NaMn <sup>III</sup> <sub>3</sub> Mn <sup>II</sup> ] clusters constructed using a multidentate Schiff-base ligand and decorated with different auxiliary ligands. New Journal of Chemistry, 2014, 38, 545-551.	2.8	11
75	Comparative study on sandwich-structured SiO <sub>2</sub> @Ag@SnO <sub>2</sub> and inverse SiO <sub>2</sub> @SnO <sub>2</sub> @Ag: key roles of shell ordering and interfacial contact in modulating the photocatalytic properties. RSC Advances, 2015, 5, 81059-81068.	3.6	11
76	Novel manganese( <scp>ii</scp> ) and cobalt( <scp>ii</scp> ) 2D polymers containing alternating chains with mixed azide and carboxylate bridges: crystal structure and magnetic properties. RSC Advances, 2016, 6, 72326-72332.	3.6	11
77	A multi-stimuli-responsive metallohydrogel applied in chiral recognition, adsorption of poisonous anions, and construction of various chiral metal–organic frameworks. Chemical Communications, 2019, 55, 14178-14181.	4.1	11
78	Two new carboxylate–oxygen bridged trinuclear M(II) (MMn and Co) compounds with zwitterionic dicarboxylate ligands: crystal structures and magnetism. Inorganic Chemistry Communication, 2015, 58, 67-70.	3.9	10
79	Steering photoinduced charge kinetics via anionic group doping in Bi <sub>2</sub> MoO <sub>6</sub> for efficient photocatalytic removal of water organic pollutants. RSC Advances, 2017, 7, 35883-35896.	3.6	10
80	A pair of enantiomeric trinuclear nickel (II) clusters based on chiral Schiff-base: Synthesis, structures, circular dichroism and magnetic properties. Inorganic Chemistry Communication, 2017, 86, 281-284.	3.9	10
81	Controlled synthesis of MOFs@MOFs core–shell structure for photodynamic therapy and magnetic resonance imaging. Materials Letters, 2019, 237, 197-199.	2.6	10
82	Effective enhancement of capacitive performance by the facile exfoliation of bulk metal–organic frameworks into 2D-functionalized nanosheets. Nanoscale, 2021, 13, 13273-13284.	5.6	10
83	A pair of homochiral trinuclear Zn(ii) clusters exhibiting unusual ferroelectric behaviour at high temperature. CrystEngComm, 2019, 21, 2355-2361.	2.6	8
84	Crystal structures and the ferroelectric properties of homochiral metal–organic frameworks constructed from a single chiral ligand. Dalton Transactions, 2020, 49, 10402-10406.	3.3	8
85	A valuable strategy to improve ferroelectric performance significantly <i>via</i> metallic ion doping in the lattice nodes of metal–organic frameworks. Chemical Communications, 2021, 57, 2515-2518.	4.1	8
86	Surface lattice oxygen mobility inspired peroxymonosulfate activation over Mn2O3 exposing different crystal faces toward bisphenol A degradation. Chemical Engineering Journal, 2022, 450, 138147.	12.7	8
87	Syntheses, Crystal Structures, and Magnetic Properties of μâ€O/μâ€Cl Bridged Dinuclear Manganese(II) and Copper(II) Complexes with Schiff base Ligand HL [HL = 2â€(benzothiazolâ€2â€ylâ€hydrazonomethyl)â€6â€methoxyphenol]. Zeitschrift Fur Anorganische Und Allgemein Chemie, 2011, 637, 2300-2305.	e <sup>1.2</sup>	7
88	Synthesis, characterization, and enhanced luminescence of CaWO4:Eu3+/SBA-15 composites. Journal of Materials Science, 2012, 47, 6305-6314.	3.7	7
89	Metallo-supramolecular grid-type architectures for highly and selectively efficient adsorption of dyes in water. RSC Advances, 2015, 5, 43334-43337.	3.6	7
90	Construction and crystal structure of a pair of tetranuclear Zn(II) chiral clusters that exhibit ferroelectric behavior under a higher frequency electric field at room temperature. Polyhedron, 2017, 137, 217-221.	2.2	7

#	Article	IF	CITATIONS
91	Structure engineering of lanthanide functionalized metal-organic frameworks: A versatile tool for the early diagnosis of pheochromocytomas and paragangliomas. Spectrochimica Acta - Part A: Molecular and Biomolecular Spectroscopy, 2022, 264, 120263.	3.9	7
92	Post-synthetic modification within MOFs: a valuable strategy for modulating their ferroelectric performance. CrystEngComm, 2022, 24, 724-737.	2.6	7
93	Multicomponent TiO <sub>2</sub> /Ag/Cu <sub>7</sub> S <sub>4</sub> @Se Heterostructures Constructed by an Interface Engineering Strategy for Promoting the Electrocatalytic Nitrogen Reduction Reaction Performance. Inorganic Chemistry, 2022, 61, 7165-7172.	4.0	7
94	Cu, Ag–containing systems based on coal gangue as catalysts for highly efficient antibiotics removal via persulfate activation under visible light irradiation. Journal of Environmental Chemical Engineering, 2021, 9, 105016.	6.7	6
95	A Novel Luminescent Metalâ€Organic Framework as a Remarkable Sensor for Detecting Aristolochic Acids in Biological Fluids. European Journal of Inorganic Chemistry, 2021, 2021, 1695-1700.	2.0	6
96	A new cobalt coordination framework based on trinuclear Co(II)-tetrazolate bridges and a terpyridine tetrazolate ligand: Synthesis and magnetism. Inorganic Chemistry Communication, 2019, 107, 107465.	3.9	5
97	An unusual high-frequency ferroelectric obtained via the post-synthetic modification of a metal–organic framework. Dalton Transactions, 2020, 49, 10895-10900.	3.3	5
98	Significant improvement of the lithium-ion conductivity of solid-state electrolytes by fabricating large pore volume hollow ZIF-8. Dalton Transactions, 2021, 50, 13877-13882.	3.3	5
99	Efficient improvement of the lithium ionic conductivity for a polymer electrolyte <i>via</i> introducing porous metal–organic frameworks. Chemical Communications, 2022, 58, 6717-6720.	4.1	4
100	A novel lithium-impregnated hollow MOF-based electrolyte realizing an optimum balance between ionic conductivity and the transference number in solid-like batteries. Journal of Materials Chemistry A, 2022, 10, 14020-14027.	10.3	4
101	Zinc(II) and Cadmium(II) Complexes Based on 4,5â€Di(4′â€carboxylphenyl)phthalic Acid Ligand: Synthesis, Crystal Structure, and Luminescent Properties. Zeitschrift Fur Anorganische Und Allgemeine Chemie, 2014, 640, 1782-1788.	1.2	3
102	An unusual homospin Co <sup>II</sup> ferrimagnetic single-chain magnet with large hysteresis. CrystEngComm, 2019, 21, 6958-6963.	2.6	3
103	Three New Metal–Organic Polymers Based on Flexible 3-(4-(Carboxymethoxy) Phenyl) Propanoic Acid: Crystal Structures, Luminescent and Magnetic Properties. Journal of Inorganic and Organometallic Polymers and Materials, 2013, 23, 1347-1353.	3.7	2
104	Modulating the ferroelectric performance by altering halogen anions in the crystals of tetranuclear copper-clusters. New Journal of Chemistry, 2021, 45, 12091-12096.	2.8	1